Viscoelastic Properties and Dynamics of Porcine Gastric Mucin

ARTICLE *in* BIOMACROMOLECULES · MARCH 2005

Impact Factor: 5.75 · DOI: 10.1021/bm0493990 · Source: PubMed

Viscoelastic Properties and Dynamics of Porcine Gastric Mucin

Jonathan Celli,[†,‡] Brian Gregor,[†,‡] Bradley Turner,[§] Nezam H. Afdhal,[§] Rama Bansil,*[,†] and Shyamsunder Erramilli*[,†]

Department of Physics, Boston University, Boston, Massachusetts 02215, and Division of Gastroenterology, Beth Israel Deaconess Medical Center and Harvard Medical School, Boston, Massachusetts 02215

Received September 22, 2004; Revised Manuscript Received January 20, 2005

Gastric mucin is a glycoprotein known to undergo a pH-dependent sol−gel transition that is crucial to the protective function of the gastric mucus layer in mammalian stomachs. We present microscope-based dynamic light scattering data on porcine gastric mucin at pH 6 (solution) and pH 2 (gel) with and without the presence of tracer particles. The data provide a measurement of the microscale viscosity and the shear elastic modulus as well as an estimate of the mesh size of the gel formed at pH 2. We observe that the microscale viscosity in the gel is about 100-fold *lower* than its macroscopic viscosity, suggesting that large pores open up in the gel *reducing* frictional effects. The data presented here help to characterize physiologically relevant viscoelastic properties of an important biological macromolecule and may also serve to shed light on diffusive motion of small particles in the complex heterogeneous environment of a polymer gel network.

Introduction

It is generally believed that aggregation/gelation of the mucus layer plays a critical role in the famous auto-digestion paradox:[1] the ability of the stomach to not be digested by the digestive gastric juice it secretes. Mucus, in general, is a complex secretion consisting of approximately 95% water, 3% mucin glycoprotein, and 2% other small molecules. The viscoelastic and polyelectrolytic properties of gastric mucin, a high molecular weight glycoprotein with a complex bottle-brush structure of polysaccharide chains on a protein core, are most likely responsible for the protective ability of gastric mucus.[2−5]

Dynamic light scattering (DLS) studies[6,7] of purified porcine gastric mucin (PGM) have shown that a pH-dependent conformational change leads to gelation at a pH less than approximately 4 when the concentration is greater than 10 mg/mL. The mechanism of gelation and pH dependence of the rheological properties of gastric mucin are not well understood. In an effort to address how the rheology of mucin changes with pH we report results of probe diffusion measurements on PGM at the physiologically relevant pH values of 2 and 6 at a concentration of 12 mg/mL, using a microscope-based DLS instrument. Though it is desirable to perform measurements on human gastric mucin, PGM has been widely studied as a model system due to the anatomy and physiology similarities between pig and human stomachs and sequence similarity between PGM and human gastric mucin MUC5AC.[5] Prior studies on PGM have used multiple particle tracking methods on reconstituted PGM[8] and human cystic fibrotic (CF) sputum mucin.[9,10] However, the use of reconstituted mucin purchased from commercial vendors as a model for natural gastric mucin has been called into question.[11] In this work, we have used purified PGM. The use of a microscope allows DLS data acquisition from a sampled volume as small as 8 pL and requires only 10−15 μL of total sample volume. These experiments provide a measurement of the local microscale viscosity and the shear elastic modulus in the gel state, as well as an estimate of the mesh size of the gel formed at pH 2.

Experimental Section

Materials. Experiments were performed on purified PGM that is more physiologically relevant than commercially available degraded gastric mucin that does not form a gel at low pH.[12] PGM was prepared using the same methods that we have used in previous studies of PGM and has been extensively characterized.[2,4−7,13−19] Briefly, this consists of first scraping the mucus layer of fresh pig stomachs and then solubilizing the scrapings by stirring overnight in 0.2 M NaCl containing 0.04% sodium azide and the protease inhibitors 5 mM benzamidine HCl, 1 mM phenylmethylsulfonylfluoride, 1 mM dibromoacetophenone, and 5 mM ethylenediaminetetraacetic acid adjusted to a pH of 7 with 1 M NaOH.[13] After centrifugation at 50 000*g* for 1 h, the supernatant containing soluble PGM was fractionated in size by Sepharose CL-2B column chromatography. Following fractionation, void volume fractions containing high molecular weight hexose positive glycoproteins were pooled and concentrated further via ultrafiltration using a filter with a 300-kDa cutoff. Purified PGM was then prepared from the concentrate by density gradient ultracentrifugation in CsCl with an initial concentration of 42% (w/w) at 300 000*g* for 24 h. The

* Corresponding authors. E-mail: shyam@bu.edu (S.E.); rb@bu.edu (R.B.).
† Boston University
‡ These authors contributed equally to this work.
§ Beth Israel Deaconess Medical Center and Harvard Medical School

10.1021/bm0493990 CCC: $30.25
Published on Web 03/30/2005

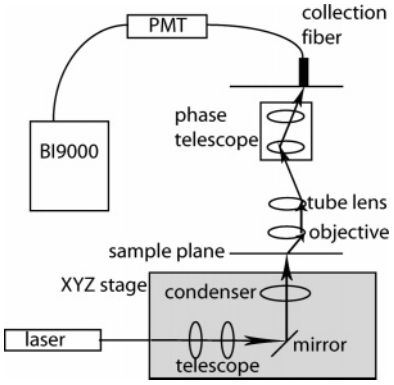

Figure 1. Schematic diagram of the microscope-based DLS apparatus where the path of light through the microscope into the photomultiplier tube (PMT) is represented with arrows. The signal from the PMT is fed into a Brookhaven Instruments correlator (BI9000) to obtain the correlation function.

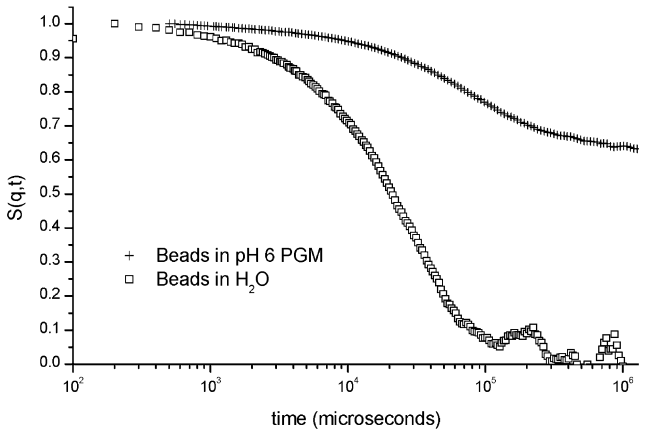

Figure 2. Representative curve showing the dynamic structure factor of 109-nm polystyrene spheres in PGM at pH 6 (+) and in deionized water (□). Both sets of data were acquired at a scattering angle of 9.6°.

densities of recovered fractions from the tops of the tubes were determined by weighing aliquots, and the glycoprotein content was determined by a micro-phenol-sulfuric hexose assay.[14] The fractions that contain glycoproteins of average density 1.45 g/mL were then pooled, dialyzed, and lyophilized for further study. PGM prepared by this method was essentially free from contaminating proteins and lipids,[15,16] and its amino acid composition[17] was typical of mucins with a predominance of the amino acid residues serine, threonine, and proline (230, 163, and 135 residues per 1000 respectively). The 10 mM phosphate-succinate buffers of varying pH were used to set the desired final pH. The physical properties of PGM in these buffers were comparable to those found in solutions of the same pH and at constant ionic strength as previously reported.[4] For probe diffusion DLS measurements, mono-sized polystyrene beads (PolySciences, Inc., Warrington, PA) of 109-nm diameter were used as tracer particles. To prepare such samples, the polystyrene beads were first mixed with Triton X-100 surfactant and added to the PGM before buffering to prevent aggregation of the beads as has been done in previous studies of the movement of beads in gels.[20] In control samples not containing any beads, an equal volume of distilled water was added to the PGM so that the final glycoprotein concentrations were the same in both cases. The samples were prepared to final concentrations of 12 mg/mL PGM, with 0.025% surfactant by mass and less than 0.005 (v/v) 109-nm polystyrene spheres. The fraction of surfactant added is sufficient to prevent sticking of the beads but does not alter the pH value at which gelation of the sample occurs. Finally, a volume of about 15 μL of sample was placed on a microscope slide that had first been cleaned by etching, using a solution of 2-propanol and KOH. A coverslip, also cleaned by the same procedure, was placed on top of the sample with a thin ring of vacuum grease to seal it.

Microscope-Based DLS. A DLS spectrometer was built on the platform of an upright microscope (Figure 1).[18] The micro-DLS design was based on a previous implementation of DLS on a microscope using an inverted microscope and a phase telescope.[20] Incident light from the TEM_{00} mode of a green helium neon laser (543.5 nm), collimated to a 100-μm beam diameter, is scattered through the objective and imaged onto the plane of a translating optical fiber by means of a phase telescope. The fiber can be positioned to detect scattered light at a scattering angle from 0 to 12°. The micro-DLS instrument has a scattering volume of about 8 pL, defined by the intersection of the beam with the depth of focus of the objective. The scattering volume for the micro-DLS instrument is about 1000 times smaller than that of a conventional DLS instrument. Additionally, the micro-DLS scattering volume is selectable by translation of the microscope stage. DLS has been used to perform microrheological studies on biological complex fluids by several groups.[20,21] Micro-DLS, because of the small scattering volume, allows the study of microrheology of more turbid samples while still in the single scattering regime and also allows for simultaneous imaging of the sample. The small total sample volume is also advantageous when the sample itself is either costly or time-consuming to prepare in large quantities. In a typical experiment, the intensity autocorrelation function, $G_2(t)$, is collected over 5 decades in time (t) from about 100 μs to 10 s. The dynamic structure factor $S(q, t)$ is obtained from the intensity autocorrelation function, $G_2(t)$, by $S(q, t) = [(G_2(t) - B)/(G_2(0) - B)]^{1/2}$, where q is the scattering vector magnitude given by $q = (4\pi n/\lambda) \sin(\theta/2)$ and B is the baseline of the measurement.

Results and Discussion

PGM at pH 6. Figure 2 shows a representative structure factor of a PGM solution at pH 6 containing tracer beads acquired at a scattering angle of 9.6°. At pH 6 the PGM is in the solution phase, and the contribution to the scattering from PGM itself is negligible compared to the scattering signal from the tracer beads. It is noteworthy that, unlike with the polystyrene beads in water, the structure factor of the beads in this entangled solution does not decay to a baseline on accessible time scales, so the curve is normalized by the calculated baseline of the autocorrelator. The inaccessibility of the baseline may be due to very slow-scale dynamics that are known to occur in entangled polymer solutions[22] as well as in polyelectrolyte solutions and mixtures.[23] A phenomenological fit to the data was made to

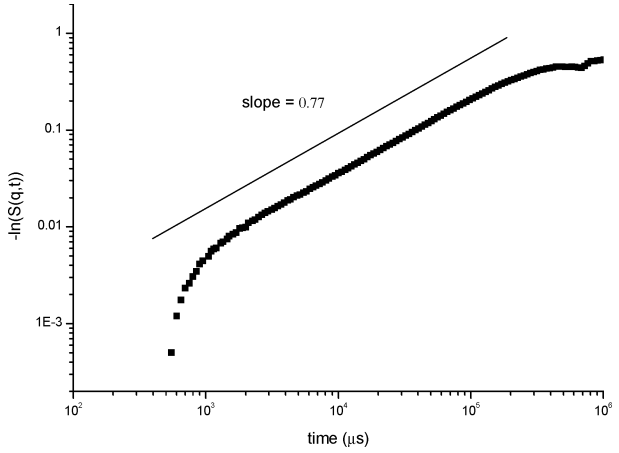

Figure 3. Using the same structure factor used in Figure 2 and plotting $-\ln[S(q, t)]$ versus time in log−log space yields a straight line fit over several decades, the slope of which is the stretching exponent $\beta = 0.77$.

the functional form

$$S(q, t) = A_1 \exp(-t/\tau_f) + A_2 \exp[-(t/\tau_s)]^{\beta} \qquad (1)$$

The fit yields the amplitude coefficients A_1 and A_2 and the time constants τ_f and τ_s. This form was inspired by the mode coupling theory (MCT) of Ngai and Phillies.[24] Briefly, MCT predicts that the system is made up of "basic units" which interact in a strong nonlinear manner. The first term represents the short-term dynamics due to density fluctuations in the solution, and the second term is a stretched exponential to describe the longer time dynamics due to the interactions of the polymer clusters. The second term reflects the polydispersity of the system and is a measure of the "width" of the distribution. We note that the "polydispersity" here refers not to the bead size distribution, because the beads we use are monodisperse. Rather the exponent represents a range of microenvironments that different beads experience. The microscopic interpretation of τ_s under such heterogeneous conditions is an open question. The exponent β has a range $0 \leq \beta \leq 1$, where a value of 1 represents a perfectly monodisperse system. In the data presented here it was found that the amplitude of the stretched exponential is more than 1 order of magnitude greater than the amplitude of the exponential term. Figure 3 shows a log−log plot of $-\ln[S(q, t)]$ corresponding to Figure 2 from which the value of β can be extracted from the slope. Analysis of several samples yields $\beta = 0.77 \pm 0.03$. From a nonlinear least-squares fit to the data, an average value of τ_s is found to be 0.342 ± 0.05 s. The diffusion constant D is related to the mean relaxation time by

$$\langle\tau\rangle = \int_0^{\infty} \exp(-t/\tau_s)\, dt = (\tau_s/\beta)\Gamma(1/\beta) = 1/Dq^2 \qquad (2)$$

Using the Stokes Einstein relation, $D = k_B T/6\pi\eta R$, where k_B is the Boltzmann constant, T is the temperature of the sample in Kelvin, and R is the radius of the polystyrene sphere (54.5 nm), the viscosity η of the beads local environment can be measured. At pH 6, η is found to be 3.5 $\pm$ 0.5 cP, 3.5 times that of water at the same temperature.

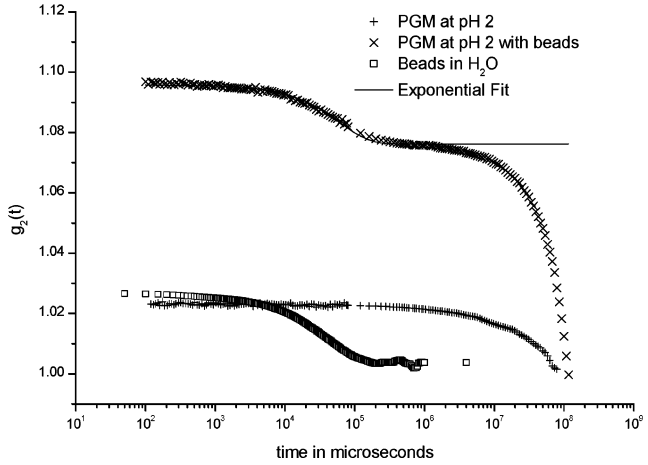

Figure 4. Intensity autocorrelation data normalized to calculate the baseline for PGM at pH 2 with (×) and without (+) 109-nm polystyrene tracer spheres, acquired at a 9.6° scattering angle. These data are shown as intensity autocorrelation rather than dynamic structure factor because, in the latter case, information about dynamic amplitude scales out. Note the similarity of the slow decay of the particles in the gel (×) with the gel alone (+) and of the fast mode (which is fit to an exponential decay) to the beads in water (□).

PGM at pH 2. At pH 2 and a concentration of 12 mg/mL, PGM is in the well-gelled state. Here, there is a significant scattering signal from both the gel itself and the beads in the gel as can be seen in Figure 4. The analysis framework used in the sol state at pH 6 cannot be used in the gel state because the system can no longer be described as interacting polymer clusters but rather a macromolecular network. The pure gel scattering provides information about the slow relaxation dynamics of the gel alone and serves as a control to allow for the extraction of that portion of the structure factor resulting from the beads alone. From the pH 2 PGM with beads curve in Figure 4, it can be seen that there are two distinct time scales: a fast exponential decay and a slower nonexponential mode. The former is nearly identical to the decay of the control sample of tracer beads in water, while the latter strongly resembles the decay seen in the pure gel sample but with a significantly higher scattering amplitude. From this we conclude that the beads contribute to the total dynamic structure factor both by relatively free diffusive motion within the fluid-filled pores of the gel and by moving with the gel, in effect amplifying the scattering intensity from the slow decay mode of the gel matrix. In other words, since the gel is highly heterogeneous, containing a wide distribution of pore sizes, some beads end up in regions where they are relatively free to move around whereas others are trapped in very small pores.

The structure factors are fit to single exponential decays at short times, where the baseline of the measurement is the intermediate plateau from about 10^5 to 10^6 μs in Figure 4. By this method, mean values of $3.6 \times 10^{-12} \pm 0.9 \times 10^{-12}$ m^2/s for the diffusion constant and 1.1 ± 0.3 cP for the local viscosity are obtained. This value is approximately 2 orders of magnitude lower than previous macroscopic measurements of the viscosity of PGM.[4] However, this result is consistent with recent studies on the diffusion of 100 and 200-nm particles in CF sputum in which it was observed that these particles diffusing in small fluid-filled pores experience a microviscosity 7- and 15-fold smaller than the macroscopic

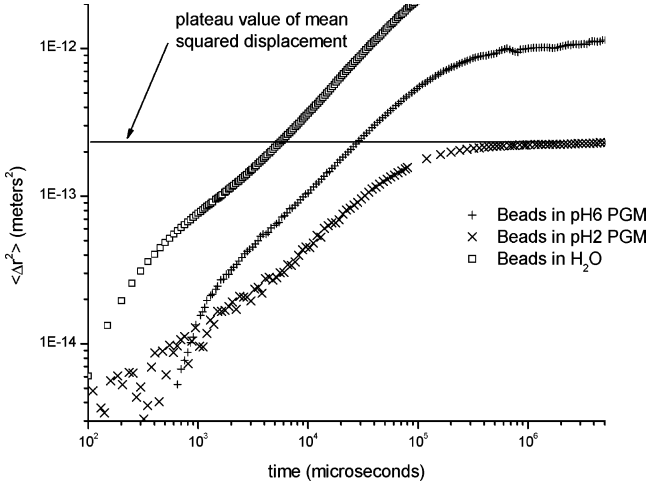

Figure 5. Mean squared displacement of beads in PGM at pH 6 (+) and pH 2 (×) and in distilled water (□), where the mean squared displacement is obtained from the structure factor by $\langle \Delta r^2 \rangle = -6 \ln[S(q, t)]/q^2$. Using the saturation value to solve for the low-frequency limit of the elastic shear modulus yields 9.4 ±1 dyn/cm^2 for pH 2 PGM.

viscosity of CF sputum, respectively.[9] Translating the microscope stage to select different microscopic scattering volumes within the same sample reveals the highly heterogeneous nature of PGM at pH 2 as the static light scattering intensity varies from point to point. This detail would be obscured in a conventional DLS experiment where the large scattering volume would average out these effects. The uncertainty in the numbers above is primarily due to the fact that these quantities deviate from point to point throughout a given sample. A preliminary analysis of these data by the method of Pusey et al.[25] for interpreting DLS data from nonergodic media agrees closely with the results here.

Additionally, an analysis protocol based on simulations of Brownian particles in microscopic cages[26] can be used to relate the baseline of the dynamic structure factor to the cage size of the gel. This analysis relates the baseline to q^2 and cage size, ξ^2, by

$$B = \exp(-q^2\xi^2) \tag{3}$$

Applying this analysis to structure factors obtained for tracer beads in pH 2 PGM reveals a range of pore sizes for the gel for selected scattering volumes at various points in various samples from about 400 to 650 nm. These results are comparable in magnitude with tapping mode atomic force microscopy (AFM) measurements of purified PGM at pH 2 spin coated onto mica disks as well as AFM measurements on human mucus samples obtained from endoscopies,[19] in which a cage size of around 200−400 nm is observed.

Finally, the mean squared displacement of beads in PGM at both pH values (pH 2 and pH 6) is shown in Figure 5. From the saturation in MSD due to confinement by the entangled polymers, the low-frequency elastic shear modulus is found to be 9.4 ± 1 dyn/cm^2 for pH 2 PGM, where the low-frequency elastic shear modulus, G, is related to the saturation value of MSD, $\langle \Delta r^2 \rangle_{max}$, by[27]

$$\langle \Delta r^2 \rangle_{max} = 3k_BT/\pi RG \tag{4}$$

These results are consistent with previous macroscopic rheology measurements of native pig gastric mucus gel[28] (55 mg/mL mucin concentration), in which the low-frequency measurements of the storage modulus are about 1 order of magnitude higher than the results here, as is expected given the approximately three times higher concentration of mucin in the native gel. The limiting value of the mean square displacement can be compared with a characteristic cubic cage of size L, using $\langle \Delta r^2 \rangle = 3L^2$. This gives $L \approx 270$ nm at pH 2. The data at pH 6 shows just the beginning of a plateau at the largest times, tending toward a higher value of the plateau than at pH 2. The estimate of L at pH 2 is comparable to that of the mesh size obtained from the dynamic amplitude data.

Conclusions

We have shown that micro-DLS is a useful probe of microrheology in a complex biological system and reported quantitative values for viscoelastic properties at two different values of pH for gastric mucin. These values help to improve characterization of a poorly understood glycoprotein that is responsible for the protective function of the mucus layer in mammalian stomachs. In a soft gel such as PGM, particles actually gain more local mobility when the polymer solution becomes cross-linked because relatively large water-filled pores open up. This observation is consistent with recent studies of the motion of 100- and 200-nm particles in CF sputum.[9,10] In contrast, when the PGM is in the solution phase the particles are uniformly hampered in their diffusive motion by the viscous polymer solution. This counter-intuitive observation may have more fundamental importance to biological gels in general.

Acknowledgment. We gratefully acknowledge support from the National Science Foundation (DBI-0242697) and the Department of Defense.

References and Notes

(1) Bernard, C. *Lecons de Physiologie experimentale appliquee a la medicine*; Balliere: Paris, 1856.
(2) Bansil, R.; Stanley, E.; Lamont, J. T. Mucin Biophysics. *Annu. Rev. Physiol.* **1995**, *57*, 635−657.
(3) Montreuil, J.; Vliegenthart, J. F. G.; Schacter, H. *Glycoproteins*; Elsevier: New York, 1995.
(4) Bhaskar, K. R.; Gong, D.; Bansil, R.; Pajevic, S.; Hamilton, J. A.; Turner, B. S.; Lamont, J. T. *Am. J. Physiol.* **1991**, *261*, G827−G832.
(5) Turner, B. S.; Bhaskar, K. R.; Hadzopoulou-Cladaras, M.; LaMont, J. T. *Biochim. Biophys. Acta* **1999**, *1447*, 77−92.
(6) Cao, X.; Bansil, R.; Bhaskar, K. R.; Turner, B. B.; LaMont, J. T.; Niu, N.; Afdhal, N. H. *Biophys. J.* **1999**, *76*, 1250−1258.
(7) Cao, X. Ph.D. Thesis, Boston University, Boston, MA, 1997.
(8) Dawson, M.; Krauland, E.; Wirtz, D.; Hanes, J. *Biotechnol. Prog.* **2004**, *20*, 851−857.
(9) Dawson, M.; Wirtz, D.; Hanes, J. *J. Biol. Chem.* **2003**, *278*, 50393−50401.
(10) Suh, J.; Dawson, M.; Hanes, J. *Adv. Drug Delivery Rev.* **2005**, *57*, 63−78.
(11) Kocevar-Nared, J.; Kristl, J.; Smid-Korbar, *J. Biomat.* **1997**, *18*, 677−681.
(12) Waigh, T. A.; Papagiannopoulos, A.; Voice, A.; Bansil, R.; Unwin, A. P.; Dewhurst, C. D.; Turner, B.; Afdhal, N. *Langmuir* **2002**, *18*, 7188−7195.
(13) Allen, A.; Pearson, J. P.; Hutton, D. A.; Mall, A. H.; Coan, R. M.; Sellers, L. A. *Symp. Soc. Exp. Biol.* **1989**, *43*, 241−248.
(14) Fox, J. D.; Robyt, J. F. *Anal. Biochem.* **1991**, *30*, 93−96.
(15) Grisham, M.; von Ritte, C.; Smith, B.; Lamont, J.; Grnager, D. *Am. J. Physiol.* **1987**, *253*, G93−G96.

(16) Gong, D.; Turner, B.; Bhaskar, K.; Lamont, J. *Am. J. Physiol.* **1990**, *259*, G681−G686.
(17) Turner, B.; Bhaskar, K.; Hadzopoulou-Cladaras, M.; Specian, R.; Lamont, J. *Biochem. J.* **1995**, *308*, 89−96.
(18) Gregor, B. Ph.D. Thesis, Boston University, Boston, MA, 2004.
(19) Hong, Z. Ph.D. Thesis, Boston University, Boston, MA, 2004.
(20) Kaplan, P. D.; Weitz, D. A. *Appl. Opt.* **1999**, *38*, 4151−4157.
(21) Tseng, Y.; Fedorov, E.; McCaffery, M.; Almo, S. C.; Wirtz, D. *J. Mol. Biol.* **2001**, *310*, 351−366.
(22) de Gennes, P. G.; Leger, L. *Annu. Rev. Phys. Chem.* **1982**, *33*, 49−61.
(23) Sedlak, M. *Langmuir* **1999**, *15* (12), 4045−4051.
(24) Ngai, K. L.; Phillies, G. D. J. *J. Chem. Phys.* **1996**, *105*, 8385−8397.
(25) Pusey, P. N.; van Meegan, W. *Physica A* **1989**, *157*, 705.
(26) Konak, C.; Konak, M.; Bansil, R. *Physica A* **1991**, *171*, 19−25.
(27) Mason, T. G.; Weitz, D. A. *Phys. Rev. Lett.* **1995**, *74*, 1250−1253.
(28) Sellers, L. A.; Allen, A.; Morris, E. R.; Ross-Murphy, S. B. *Biorheology* **1987**, *24*, 615−623.

BM0493990